



LETTER • OPEN ACCESS

Atmospheric precursors to the Antarctic sea ice record low in February 2022

To cite this article: Juhi Yadav *et al* 2022 *Environ. Res. Commun.* 4 121005

View the [article online](#) for updates and enhancements.

You may also like

- [Spring–summer albedo variations of Antarctic sea ice from 1982 to 2009](#)
Zhu-De Shao and Chang-Qing Ke
- [An ocean-sea ice model study of the unprecedented Antarctic sea ice minimum in 2016](#)
Kazuya Kusahara, Phillip Reid, Guy D Williams *et al.*
- [Contribution of the deepened Amundsen sea low to the record low Antarctic sea ice extent in February 2022](#)
Shaoyin Wang, Jiping Liu, Xiao Cheng *et al.*



LETTER

Atmospheric precursors to the Antarctic sea ice record low in February 2022

OPEN ACCESS

RECEIVED
8 July 2022REVISED
11 November 2022ACCEPTED FOR PUBLICATION
24 November 2022PUBLISHED
12 December 2022

Original content from this work may be used under the terms of the [Creative Commons Attribution 4.0 licence](#).

Any further distribution of this work must maintain attribution to the author(s) and the title of the work, journal citation and DOI.

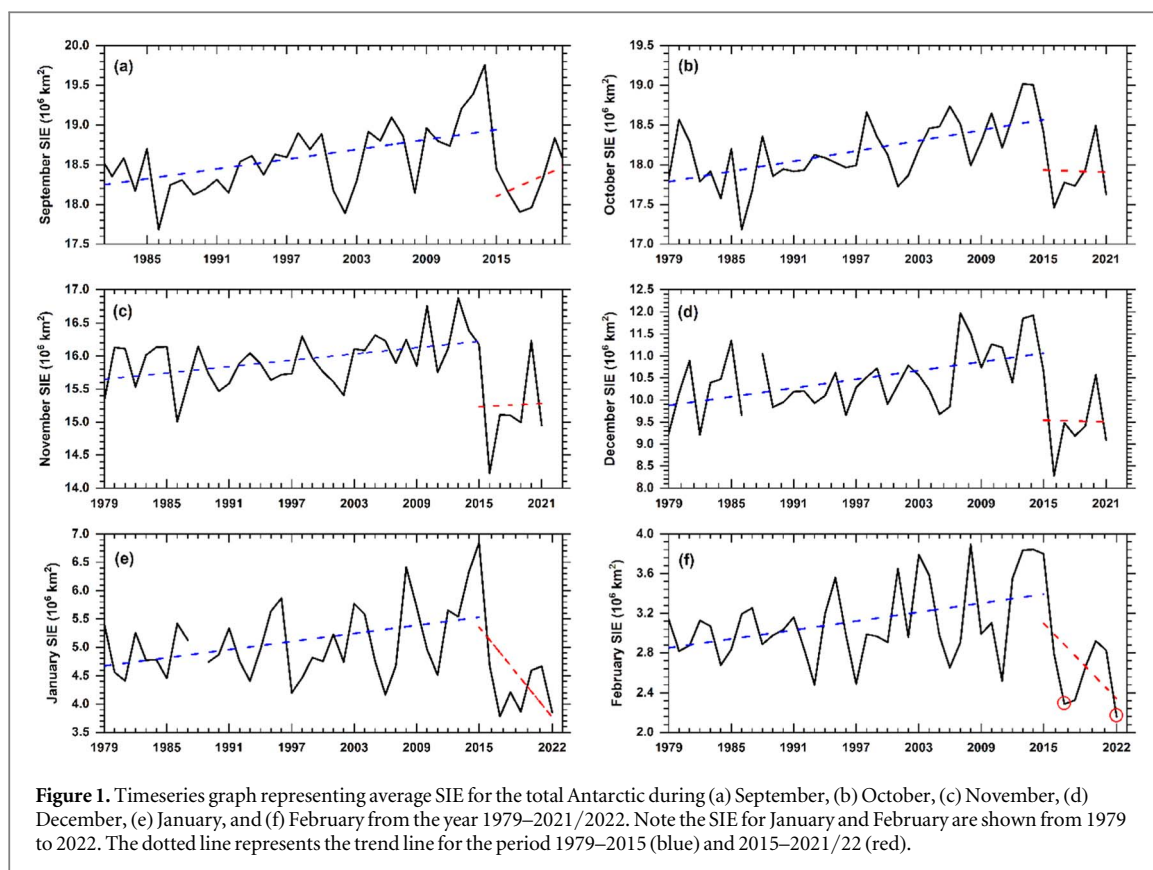
Juhi Yadav^{1,2} , Avinash Kumar¹  and Rahul Mohan¹ ¹ National Centre for Polar and Ocean Research, Ministry of Earth Sciences, Govt. of India, Goa, India² Department of Marine Geology, Mangalore University, Mangalore, IndiaE-mail: avinash@ncpor.res.in**Keywords:** sea ice decline, sea ice concentration, Amundsen sea low, Southern annular mode, Weddell seaSupplementary material for this article is available [online](#)

Abstract

Antarctic sea ice expansion and recession are asymmetric in nature, with regional and temporal variations. The decade-long overall increase in the Antarctic sea ice extent (SIE) until 2015 showed a decrease in recent years since satellite records were available. The present study focused on determining the atmospheric forcing and climate fluctuations responsible for the lowest SIE record in February 2022. Here, the lowest SIE record was assumed to result from the sea ice recession that began in September 2021. The SIE reached a record low of $2.16 \times 10^6 \text{ km}^2$ in February 2022, which was 43% lower than the mean extent of the previous February months since the satellite era. However, the second-lowest SIE was recorded from November 2021 to January 2022. The Weddell Sea, Ross Sea, and Bellingshausen/Amundsen Seas (ABS) sectors experienced the maximum sea ice change on a regional scale. The record-low SIE occurred when the Amundsen Sea Low (ASL) pressure center was intensified, with the Southern Annular Mode (SAM) at its positive phase. Together, these two climate fluctuations played a role in modifying the pressure and wind patterns in Antarctica. The warm northerly winds largely contributed to decreased SIE. Further, the study investigated the Polar Cap Height (PCH), which demonstrates a strengthening of the stratospheric polar vortex and positive polarity of the SAM.

1. Introduction

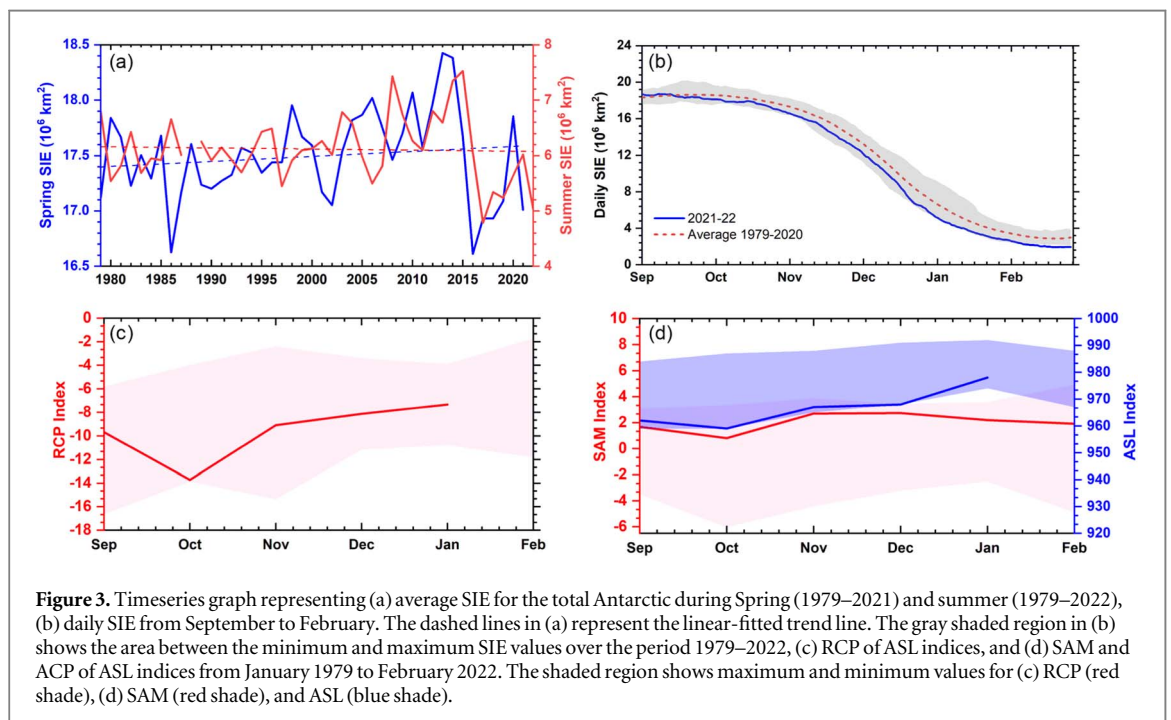
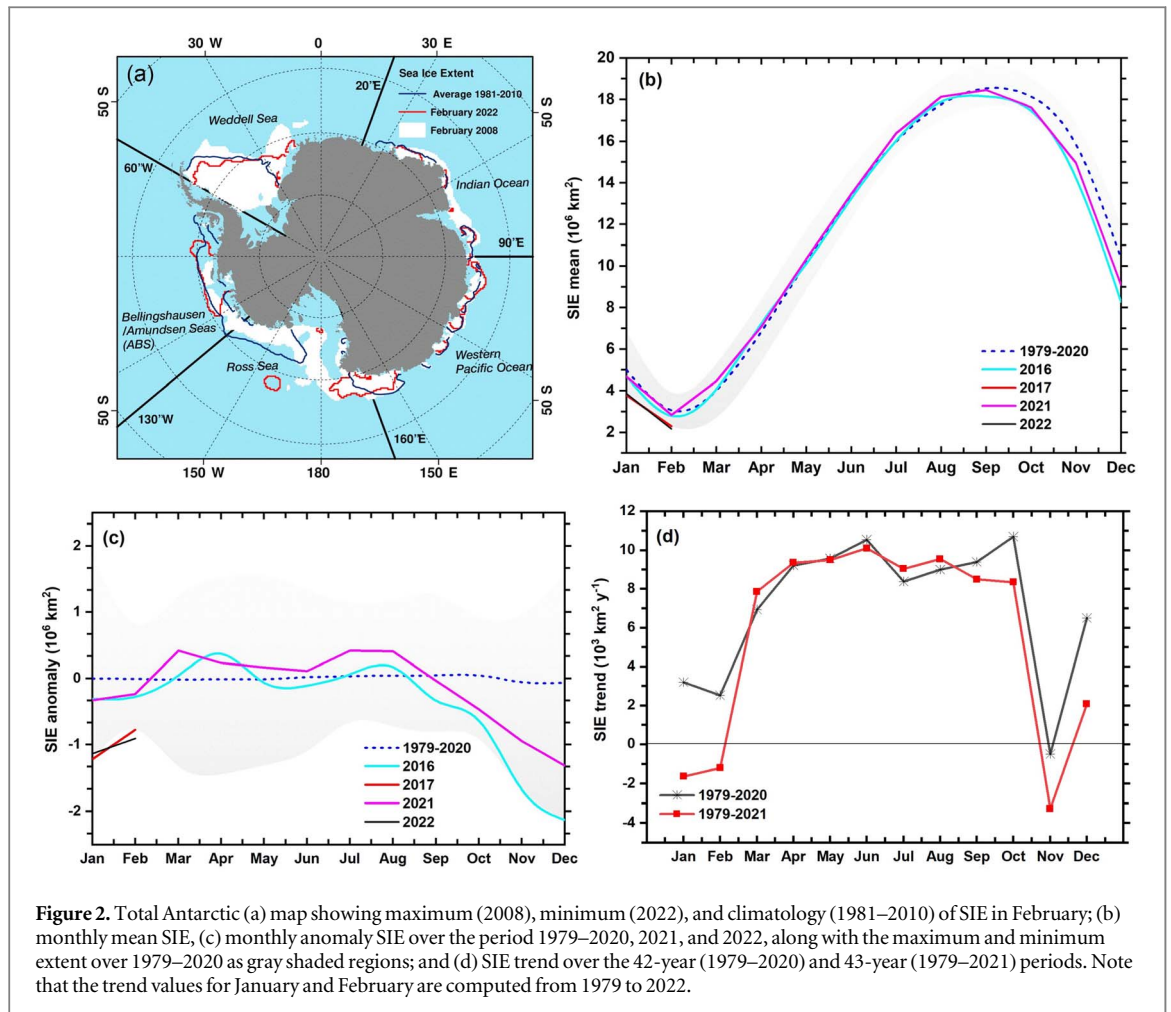
Polar sea ice fluctuation is an essential component of the complex global climate system, as it can reflect and affect other climatic components of the system (Eayrs *et al* 2019, 2021). The advent of satellite remote sensing in the late 1970s enabled the continuous observation of sea ice distribution in remote and harsh polar environments with higher spatiotemporal coverage (Parkinson and Cavalieri 2012). Since 1979, the Antarctic sea ice extent (SIE) has shown a weak but significant positive trend until 2015, when it unexpectedly declined by ~50%, with no discernible trend in subsequent years (Kusahara *et al* 2018, Parkinson 2019). The Antarctic annual mean SIE decreased by $2.03 \times 10^6 \text{ km}^2$ between 2015–2017 (Simmonds and Li 2021). However, Antarctic sea ice variability is regional and seasonal in nature (Zwally *et al* 2002, Meehl *et al* 2019), as sea ice cover changes rapidly, and approximately 15 million km^2 of ice forms and melts each year (Eayrs *et al* 2019). Since the satellite era, the overall decade-long weak positive Antarctic SIE trend has been explained by several mechanisms (Turner and Overland 2009, Holland *et al* 2017). These mechanisms include freshening and cooling of the Southern Ocean surface due to decreased upwelling of warmer water (Bintanja *et al* 2013, Armour *et al* 2016, Purich *et al* 2018), strengthening of the westerly wind belt due to the Southern Annular Mode (SAM) (Pezza *et al* 2012, Comiso *et al* 2017, Doddridge and Marshall 2017), and changes in the Amundsen Sea Low (ASL) pressure center in Antarctica, resulting in variations in sea ice concentration (SIC) and transport anomalies (Turner *et al* 2015, Holland *et al* 2018). The ASL is a low-pressure system in the Southern Ocean that traverses across the Ross Sea and



Bellingshausen–Amundsen Sea sectors, resulting in warmer conditions and increased northerly wind anomalies (Donat–Magnin *et al* 2020). The Antarctic SIE is influenced by atmospheric circulation through the process of sea ice drift and atmospheric heat transport, which are induced by climatic modes. In addition, the surface climatic variations are linked to the stratosphere–troposphere coupling processes. The earlier studies demonstrated a linkage between the stratospheric polar vortex and the low springtime SIE record in 2016 (Wang *et al* 2019, 2021).

Since the availability of satellite records, the yearly average of the total Antarctic SIE had a maximum extent of $12.8 \times 10^6 \text{ km}^2$ in 2014 and a minimum of $10.7 \times 10^6 \text{ km}^2$ in 2017 (Parkinson 2019). Over the first three decades, the Antarctic SIE showed a gradual increase, followed by a sharp decrease from 2015 onward (Cerrone *et al* 2017, Eayrs *et al* 2021). The Antarctic SIE trend from 1979–2015 was significantly positive from September to February at 95% and 99% significance levels (table S1). The trend analysis shows a positive trend from September to February in the Indian Ocean sector, western Pacific Ocean sector, and Ross sea, while a negative trend persisted in the ABS and the Weddell Sea sector. Since 2016, the maximum SIE loss has been recorded from September to February (figure 1). In addition, the second-lowest monthly SIE was recorded in 2017 ($2.29 \times 10^6 \text{ km}^2$) after the maximum sea ice recession in the spring of 2016 (Turner *et al* 2017, Wang *et al* 2019). A negative trend was observed from December to February for 2015–2021/22 (figures 1(c), (d)). The annual cycle of monthly Antarctic SIE always shows an increase in September and a decrease in February (Parkinson 2019). During February 2022, Antarctic sea ice recorded an unprecedented record low SIE ($2.16 \times 10^6 \text{ km}^2$) (figures 2(a)–(c)). Notably, the difference between the maximum February Antarctic SIE of 2008 ($3.9 \times 10^6 \text{ km}^2$) and the minimum Antarctic SIE of 2022 was only $1.74 \times 10^6 \text{ km}^2$ (Turner *et al* 2022).

Similarly, from October 2021 to January 2022, the Antarctic SIE was close to the minimum sea ice record since 1979 (figures 2(b), (c), and 3). As shown in figure 2(c), the SIE anomaly for January and February 2022 is very close to the lowest record set in 2017 (figure 2(c)). Based on the monthly SIE trend from 1979–2021/22, November has the highest negative trend, followed by January (figure 2(d)). In addition, the austral summer SIE, the highest minimum, was recorded in 2017 ($4.7 \times 10^6 \text{ km}^2$), followed by the second lowest record in 2022 ($5 \times 10^6 \text{ km}^2$) (figure 3(a)). The recent low sea ice records in the Antarctic may indicate the beginning of a protracted sea ice recession in the coming years, as observed in the Arctic, or it may reverse after these short-term variations (Fogt *et al* 2022, Raphael and Handcock 2022). Here, we investigated the temporal and spatial evolution of the low Antarctic sea ice record in February 2022 since the satellite record began (figure 1(f)). This study examines the monthly (September to February) and seasonal (spring and summer) sea ice variability in response



to climate changes and polar vortex variability. We studied atmospheric variables to determine their fidelity to the sea ice. Furthermore, we discussed the prevailing atmospheric conditions from September 2021 that may have contributed to the new record low SIE of February 2022.

2. Materials and method

This study analyzed sea ice data derived from multichannel passive microwave satellites since the late 1970s. We examined daily and monthly sea ice data from the United States National Snow and Ice Data Centre (<https://nsidc.org/>) generated using the NASA Team algorithm (Cavalieri *et al* 1996, Cavalieri and Parkinson 2012). Once the data from each sensor were received, they were mapped onto rectangular grids superimposed on polar stereographic projections with grid squares (or pixels) of approximately $25 \text{ km} \times 25 \text{ km}$ (NSIDC 2004). Because sea ice data were available only on alternate days prior to 1987, we interpolated the missing days using data from the preceding and following days using the nearest neighbor interpolation technique. Since no daily data were available from 3 December 1987 to 12 January 1988, interpolation was not performed for these missing days. NASA's near-real-time data were used for the years 2021–2022. SIC is the percentage of the area occupied by ice compared to the reference area. Furthermore, SIE was determined as the sum of the areas of the grid squares with at least 15% ice concentration (Parkinson *et al* 1999, Zwally *et al* 2002, Serreze *et al* 2003). We evaluated the SIE variability for the entire Antarctic and its five sectors (Cavalieri *et al* 2003, Parkinson 2019). Antarctica is divided into five sectors: the Indian Ocean, Western Pacific Ocean, Ross Sea, Amundsen–Bellingshausen Sea (ABS), and Weddell Sea (figure 2(a)).

We investigated the sensitivity of ocean–atmospheric forcing on sea ice using data from the Fifth Generation European Centre for Medium-range Weather Forecasts (ECMWF) reanalysis data (ERA5; <https://www.ecmwf.int/>). ERA5 provides higher spatiotemporal resolution data for a large number of oceanic, atmospheric, and land climate variables and is the most reliable dataset for understanding recent Antarctic climate fluctuations (Tetzner *et al* 2019, Hersbach *et al* 2020). The present study used real-time monthly data updated monthly after quality verification. The datasets obtained at the surface level from ERA5 for the period 1979–2022 include SIC, mean sea level pressure (MSLP), and 10 m zonal and meridional wind components with a spatial resolution of $0.25^\circ \times 0.25^\circ$. Similarly, the ERA5 pressure level data were retrieved for Geopotential height (GPH) and temperature from the equator to the 90°S latitude. The GPH at 50 hPa and 10 hPa was used to determine the Polar Cap Height (PCH), which is averaged over the south of 65°S (Siegmond 2005). The PCH anomaly at each pressure level was normalized by its standard deviation and is unitless.

Two dominant cycles, SAM and ASL, which regulate climatic fluctuations and sea ice in the Southern Hemisphere, were studied. Both indices were obtained from <https://climatedataguide.ucar.edu/> for the period 1979–2022. The station-based SAM index is the zonal pressure difference between the Southern Hemisphere latitudes (40° and 65°) (Marshall 2003). However, the ASL is a climatological low-pressure center located towards the coastal flank of western Antarctica and over the southern Pacific Ocean. This study used the Actual Central Pressure (ACP) of the ASL index, defined as the pressure at the ASL location (Bromwich *et al* 2012, Hosking *et al* 2013). Hosking *et al* (2013) found a significant correlation ($p < 0.01$) between ACP and SAM across all seasons. The ACP is strongly associated with and influenced by large-scale variability, including both SAM and ENSO. Therefore, we have also analyzed the Relative Central Pressure (RCP), which provides a more precise influence of ASL at a regional scale (Simmonds and Wu 1993). In the present study, anomaly calculations were performed with reference to the 42-year period (1979–2020) for all of the aforementioned ocean–atmospheric variables.

3. Results and discussion

3.1. Long-term Antarctic sea ice variability

The total Antarctic SIE from September to February shows a maximum positive trend in September ($8.5 \pm 5.0 \times 10^3 \text{ km}^2 \text{ y}^{-1}$) and a minimum in February ($-1.2 \pm 5.1 \times 10^3 \text{ km}^2 \text{ y}^{-1}$) from 1979–2021/22 (table 1). The monthly total Antarctic mean SIE from September to February revealed an unprecedented loss from 2016. In 2016, SIE was the second lowest in October ($17.5 \times 10^6 \text{ km}^2$) and the lowest in November ($14.2 \times 10^6 \text{ km}^2$) and December ($8.2 \times 10^6 \text{ km}^2$) (figures 1(b)–(d)). From 1979–2021, the lowest SIEs for January ($3.7 \times 10^6 \text{ km}^2$) and February ($2.3 \times 10^6 \text{ km}^2$) were recorded in 2017 (figures 1(e), (f)).

From September to February, the monthly SIE trend for the total Southern Ocean remained positive over the 42-year (1979–2020) period, except in November, when the trend was near zero. However, the monthly trend for the 43/44-year (1979–2021/22) period was consistently lower than the 42-year SIE trend. The SIE trend (1979–2021) was 70% lower in December 2021 than the trend for the period (1979–2020). In most parts of Antarctica, January marks the beginning of the summer sea ice retreat. The second-lowest extent ($3.86 \times 10^6 \text{ km}^2$) was recorded in January 2022, with a difference of $0.08 \times 10^6 \text{ km}^2$ from the previous lowest record in 2017 (figure 2(b)).

The most negative trend of $-3.2 \pm 6.2 \times 10^3 \text{ km}^2 \text{ y}^{-1}$ was recorded in November 2021, which was nearly six times higher than the 42-year loss for the total Antarctic. September continues to be the month with the most

Table 1. Monthly and seasonal SIE trends ($10^3 \text{ km}^2 \text{ y}^{-1}$) are shown from September to February, as well as seasonally for spring and summer for the total Southern Ocean (TSO) and its five sectors in the Indian Ocean sector (IO), Western Pacific Ocean (WPO), Ross Sea (RS), Bellingshausen-Amundsen Sea (ABS), and Weddell Sea (WS) over a 44-year (1979–2021/22) period, with a 42-year (1979–2020) period in parentheses. Italics indicate statistical significance at 95% or higher, whereas boldface indicates statistical significance at 99% or higher.

SIE	September	October	November	Spring (SON)	December	January	February	Summer (DJF)
IO	2 ± 2.6 (1.8 ± 2.8)	2.6 ± 2.8 (2.8 ± 3.0)	-1.7 ± 3.6 (-1.2 ± 3.8)	1 ± 2.6 (1.1 ± 2.8)	0.3 ± 3.3 (0.1 ± 3.5)	1.6 ± 1.2 (1.6 ± 1.3)	1.7 ± 1 (1.9 ± 1.1)	2.1 ± 1.8 (2.0 ± 2.0)
WPO	1.2 ± 2.6 (1.5 ± 2.7)	1.1 ± 2.7 (2.2 ± 2.8)	-1.8 ± 2 (-1.5 ± 2.2)	0.1 ± 2.2 (0.7 ± 2.3)	1.3 ± 1.2 (1.7 ± 1.2)	1.5 ± 1.2 (2.3 ± 1.3)	2.1 ± 1.3 (3.2 ± 1.4)	1.9 ± 1.1 (2.6 ± 1.2)
RS	5.3 ± 3.4 (5.5 ± 3.6)	8 ± 3.3 (7.8 ± 3.5)	5.7 ± 3.4 (5.5 ± 3.6)	6.3 ± 3.1 (6.3 ± 3.2)	6.8 ± 4.4 (8.5 ± 4.5)	-3.1 ± 4.1 (-0.6 ± 4.3)	-5.6 ± 3 (-4.2 ± 3.3)	0.47 ± 3.4 (2.6 ± 3.6)
ABS	0.8 ± 3.4 (1.3 ± 3.6)	-0.7 ± 3.3 (-0.6 ± 3.5)	0.12 ± 3.6 (0.74 ± 3.7)	0.05 ± 3.09 (0.4 ± 3.2)	-2.9 ± 2.8 (-2.3 ± 3)	-6.8 ± 1.8 (-8.2 ± 1.8)	-8.5 ± 1.7 (-9.6 ± 1.8)	-5.9 ± 1.9 (-6.9 ± 2)
WS	-0.9 ± 4 (-0.76 ± 4.3)	-2.6 ± 4.1 (-1.5 ± 4.2)	-5.5 ± 4.2 (-4.1 ± 4.3)	-3.0 ± 3.8 (-2.1 ± 3.9)	-3.5 ± 6.6 (-1.5 ± 6.8)	5.0 ± 5.5 (8.2 ± 5.9)	9.0 ± 3.4 (11.3 ± 3.6)	5.1 ± 5.4 (7.6 ± 5.8)
TSO	8.5 ± 5.0 (9.4 ± 4.7)	8.3 ± 4.8 (10.7 ± 4.9)	-3.2 ± 6.2 (-0.5 ± 6.4)	4.5 ± 5 (6.5 ± 5.1)	2.0 ± 9.9 (6.5 ± 10.1)	-1.6 ± 8.1 (3.2 ± 8.6)	-1.2 ± 5.1 (2.5 ± 5.4)	3.7 ± 9.1 (8.1 ± 9.7)

prominent positive sea ice trend, with a change of -10% from the previous year's record. In February, the monthly trend for 44-year was $-1.2 \pm 5.1 \times 10^3 \text{ km}^2 \text{ y}^{-1}$, which is $\sim 50\%$ of the trend for 42-year (table 1). The annual sea ice cycle reveals that sea ice retreats at the highest rate in February across the total Southern Ocean, and this year, 2022, has set a new record low for the SIE since 1979 (figures 2(a), (b)).

The total Antarctic SIE reached its fifth-lowest ($17 \times 10^6 \text{ km}^2$) record in spring 2021, a difference of $0.4 \times 10^6 \text{ km}^2$ from the first lowest record in 2016 ($16.6 \times 10^6 \text{ km}^2$) (figure 3(a)). However, the average summer SIE for 2021/22 was the third-lowest ($6.1 \times 10^6 \text{ km}^2$) and was very close to the lowest values recorded in the year 1998. Overall, the summer 2022 SIE was 18.6% lower than the mean SIE over the period 1979 to 2020. Seasonally, the Antarctic SIE trend was positive in both spring ($4.5 \pm 5.0 \times 10^3 \text{ km}^2 \text{ y}^{-1}$) and summer ($3.7 \pm 9.1 \times 10^3 \text{ km}^2 \text{ y}^{-1}$) over the period 1979–2021/22. In spring 2021, the rate of change in the Antarctic SIE trend was 30% lower than the 42-year average, and in the summer of 2022, it was 54% lower. Sea ice advance and retreat occur on a distinct timescale and at different rates in each of Antarctica's five sectors. The ABS sector experienced maximum sea ice loss in September, with a 60% ($0.8 \pm 3.4 \times 10^3 \text{ km}^2 \text{ y}^{-1}$) reduction compared to the 42-year trend ($1.3 \pm 3.6 \times 10^3 \text{ km}^2 \text{ y}^{-1}$). Sea ice loss in this sector continues until December, with maximum loss in November (table 1). The Weddell Sea and Western Pacific Ocean sectors exhibited a negative trend from September to February. In addition, the Weddell Sea had the highest monthly SIE change compared to other sectors, while the Indian Ocean sector had the lowest monthly SIE change. In January and February 2022, when the Ross Sea and the Weddell Sea experienced the highest sea ice loss, the ABS sector recorded a positive SIE trend. Seasonally, during spring, the ABS and Western Pacific Ocean sectors registered maximum sea ice changes of -90% and -76% , respectively, relative to the 42-year trend. However, in summer, the maximum sea ice retreat was recorded in the Ross Sea (-83%) and Weddell Sea (-32%), while growth occurred in the ABS and the Indian Ocean sectors (table 1).

Over the period 1979–2015, the total Antarctic minimum monthly SIE in February was consistently between $3 \times 10^6 \text{ km}^2$ and $4 \times 10^6 \text{ km}^2$, with the exception of 1993 and 1997 ($2.4 \times 10^6 \text{ km}^2$) (figure 1(f)). However, the SIE was well below $3 \times 10^6 \text{ km}^2$ after 2015. Recently, the total Antarctic SIE reached a new record minimum of $2.16 \times 10^6 \text{ km}^2$ in February 2022, with a record low of $1.9 \times 10^6 \text{ km}^2$ on 25 February (figures 1(f) and 3(b)). It is worth mentioning that the sea ice retreat began in 2021, with the largest mean total SIE change occurring in December ($-7.12 \times 10^6 \text{ km}^2$) (table S2). During 1979–2020, the SIE change was consistently negative, with the exception of September, when the SIE increased by $0.26 \times 10^6 \text{ km}^2$. In contrast, in September 2021 ($-0.59 \times 10^6 \text{ km}^2$), sea ice loss was three times greater than the 42-year mean loss. The monthly difference shows that February 2022 had the largest change of 43% compared to the previous year.

Compared to other sectors, the Weddell Sea sector experienced the greatest sea ice loss in September and October and growth from January to February 2022 (table S2). This sector exhibits positive seasonal trends in summer and autumn but negative seasonal trends in winter and Spring (Kumar *et al* 2021). In October, a positive yearly rate of change was recorded only in the Ross Sea ($0.49 \times 10^6 \text{ km}^2$). However, the magnitude at which sea ice increased in the Ross Sea experienced a rapid loss in the following months compared to the previous year's mean. The western Pacific Ocean showed a negative rate of SIE change from October to February, with a maximum difference in October. The Weddell Sea experienced the highest rate of SIE change during spring ($-2.18 \times 10^6 \text{ km}^2$), followed by the ABS ($-0.86 \times 10^6 \text{ km}^2$) and the Ross Sea sectors ($-0.83 \times 10^6 \text{ km}^2$). In contrast, the Weddell Sea and ABS both recorded positive changes in summer relative to the previous year's mean loss. The Ross Sea sector recorded a maximum sea ice retreat of $-3.21 \times 10^6 \text{ km}^2$ in summer (table S2).

3.2. Sea ice loss at a record low is linked to physical forcings

3.2.1. Monthly variability

The lowest total Antarctic SIE in February was determined by comparing the monthly change in SIC, meridional and zonal wind components, and MSLP from September 2021 to February 2022 to the long-term mean of 1979–2020 (figure 5). Similarly, to understand the monthly variability in the GPH and temperature at pressure level from the equator to 90°S has been shown in figure 6. The regions with maximum negative SIC anomalies include the Weddell Sea, the western Pacific Ocean, and the Ross Sea. In contrast, positive anomalies were observed over the Indian Ocean and western ABS sector from September to November 2021 (figures 3(a), (b), and 7(a)). The MSLP anomaly is negative across the circumpolar trough with a low-pressure center in the ABS sector (figure 7(b)). The driver of anomalous low pressure is the Amundsen Sea Low (ASL), the deepest of the three climatological low pressures formed around Antarctica (Holland *et al* 2018). It is suggested that maximum inter-annual pressure variability occurs within the ABS sector (Fogt *et al* 2012). Further, the low-pressure center allows the intrusion of warm and moist air over the ABS sector by developing the atmospheric rivers (Djoumna and Holland 2021). The strength and position of the wind moving across the Southern Ocean are largely modified by the ASL (Turner *et al* 2013). The ACP and RCP indices are used here to determine the ASL index. The RCP is the difference between the central pressure and the climatological pressure of the cyclone location at a

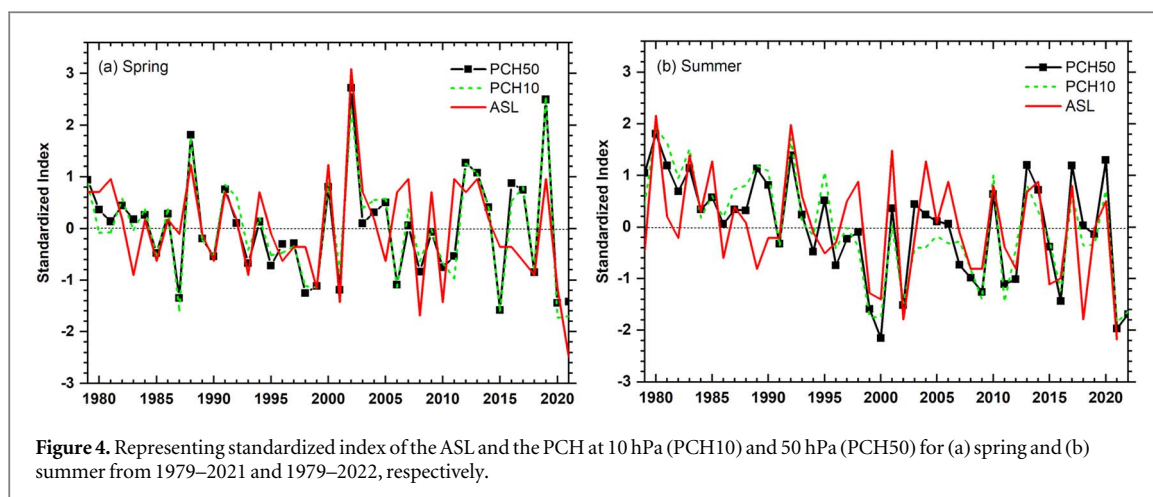


Figure 4. Representing standardized index of the ASL and the PCH at 10 hPa (PCH10) and 50 hPa (PCH50) for (a) spring and (b) summer from 1979–2021 and 1979–2022, respectively.

particular time of year (Lim and Simmonds 2002). The large-scale variability can be understood from the ACP, whereas the RCP provides accurate measurements of the regional pressure difference in West Antarctica (Hosking *et al* 2013, Raphael *et al* 2019). In this study, a monthly analysis of the RCP shows the maximum pressure difference in October (figure 3(c)). Similarly, from September to November 2021, the ACP recorded the lowest minimum pressure values in October (959 hPa) (figure 3(d)).

The ASL central pressure variations determine the temperature, surface wind patterns, downward longwave radiation, and cloud cover in the Western Antarctic (Yeung *et al* 2019). The downward longwave radiation in Antarctica regulates the sea ice variation in relation to the air and skin temperature. Since more downward longwave radiation causes higher skin temperatures and less sea ice, less radiation causes lower skin temperatures and more ice (Lee *et al* 2017, Sato and Simmonds 2021, Zhang *et al* 2021). ASL is also associated with the dominant mode of climatic fluctuations, that is, SAM. According to previous studies, SAM has been more positive over the past 30-year (Arblaster and Meehl 2006, Abram *et al* 2014, Simmonds 2015). Similarly, in the recent year 2021–2022, SAM was found to be in a positive phase, suggesting that it may intensify the westerlies and deepen the ASL. The positive and negative SAM perturbations correspond to the contraction of the westerlies towards the pole and equator, respectively (Thompson and Wallace 2000, Stuecker *et al* 2017). The phase change of the SAM was the cause of the pressure differences between higher and mid-latitudes (figures 7(b), (c)). Additionally, the stratospheric polar vortex significantly influences the ASL and SAM (England *et al* 2016, Screen *et al* 2018). Here, we have investigated the extent to which the stratospheric polar vortex modulates the climatic indices. The positive (negative) PCH anomaly corresponds to the weakening (strengthening) of the stratospheric polar vortex. The relation between the PCH50 and PCH10 with the ASL (SAM) during spring and summer shows a significantly positive (negative) correlation (table S3). Thus, indicating that a strong polar vortex is inducing positive SAM. The standardized PCH at 50 hPa and 10 hPa during spring and summer shows large inter-annual fluctuations (figure 4). During spring 2021 and summer 2022, the standardized PCH shows nearly the lowest values signifying the strengthening of the polar vortex. In 2021, the PCH10 recorded the second and third lowest values in spring and summer. In contrast, the PCH50 showed the third lowest negative value during spring 2021 and summer 2022. Consequently, the positive SAM is associated with strong westerlies, as demonstrated in figure 5.

On the other hand, the deepening of the ASL is identified with the strong northerly winds across the ABS and the Weddell Sea sectors, resulting in sea ice retreat (figures 3 and 7(d)). Meanwhile, wind-driven positive sea ice anomalies were observed in sectors with increasing southerly winds. The ABS and the Weddell Sea sectors recorded the maximum sea ice retreat from September to November (figure 7(a)). However, November 2021 had the lowest negative SIE trend, which may be the result of sea ice retreats in the western Antarctic and western Pacific Oceans. The sea ice retreat in western Antarctica is affected by shifting the low-pressure center from the western to the eastern flank of the ABS sector. In the Ross Sea, a positive SIC anomaly was observed during November and December, which was partially explained by the deepening of the ASL and strong southerly winds off the Ross Ice Shelf (figures 5(b), (c)). Similarly, warmer northwesterly winds pushed sea ice in the Indian Ocean and western Pacific sectors, resulting in positive (ice compaction towards the coast) and negative SIC anomalies off the coast. Further, the zonal mean temperature and GPH anomaly are illustrated at different pressure levels in figure 6 using the vertical-latitude section. It is evident from the figure that a positive temperature anomaly persisted below 500 hPa in the region extending from the equator towards the pole. In the months of September and October, a warm air mass from the upper stratosphere is advancing towards the surface and influencing the negative GPH anomaly center towards the pole (figures 6(a), (b)). There is a positive temperature anomaly on the

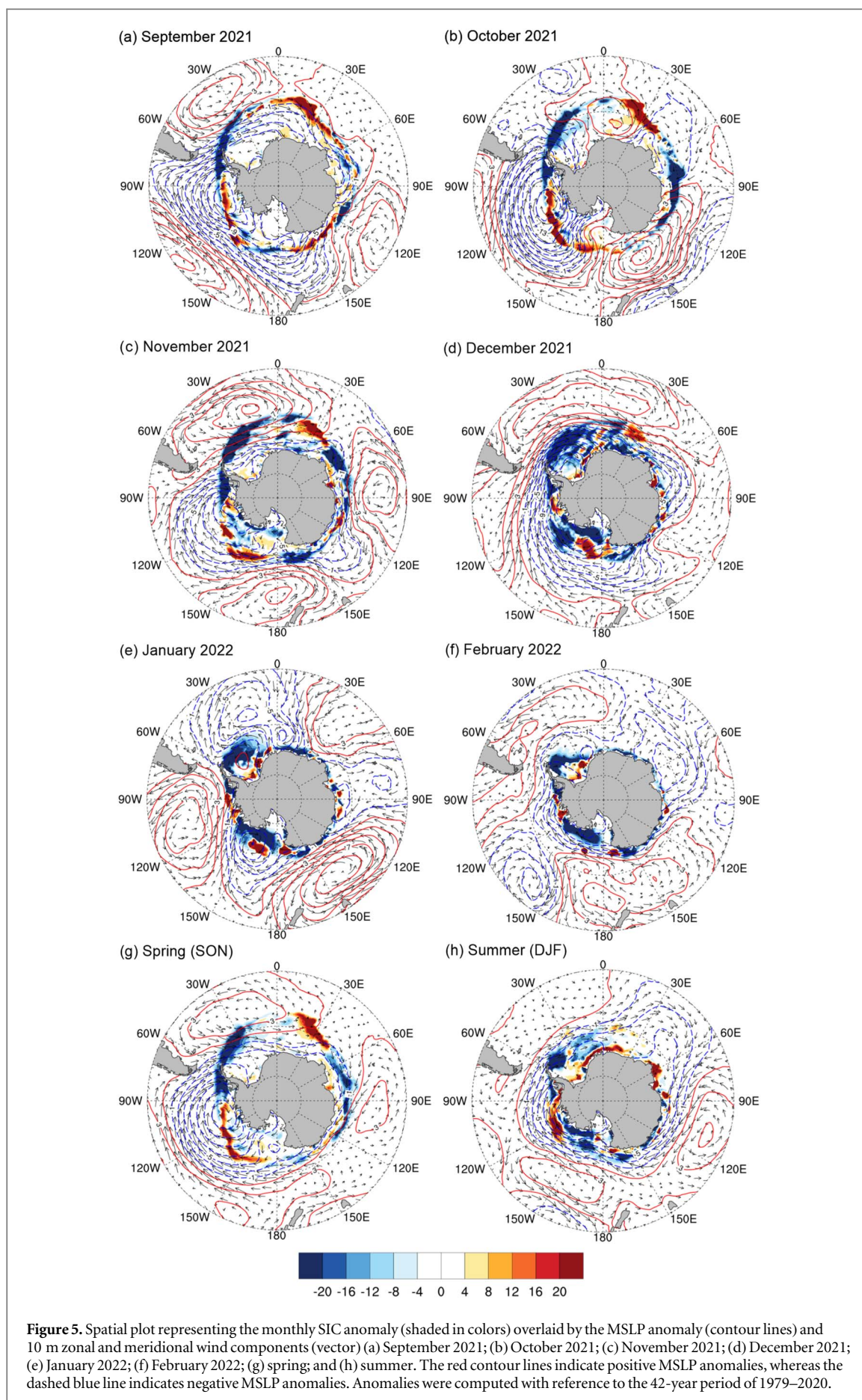


Figure 5. Spatial plot representing the monthly SIC anomaly (shaded in colors) overlaid by the MSLP anomaly (contour lines) and 10 m zonal and meridional wind components (vector) (a) September 2021; (b) October 2021; (c) November 2021; (d) December 2021; (e) January 2022; (f) February 2022; (g) spring; and (h) summer. The red contour lines indicate positive MSLP anomalies, whereas the dashed blue line indicates negative MSLP anomalies. Anomalies were computed with reference to the 42-year period of 1979–2020.

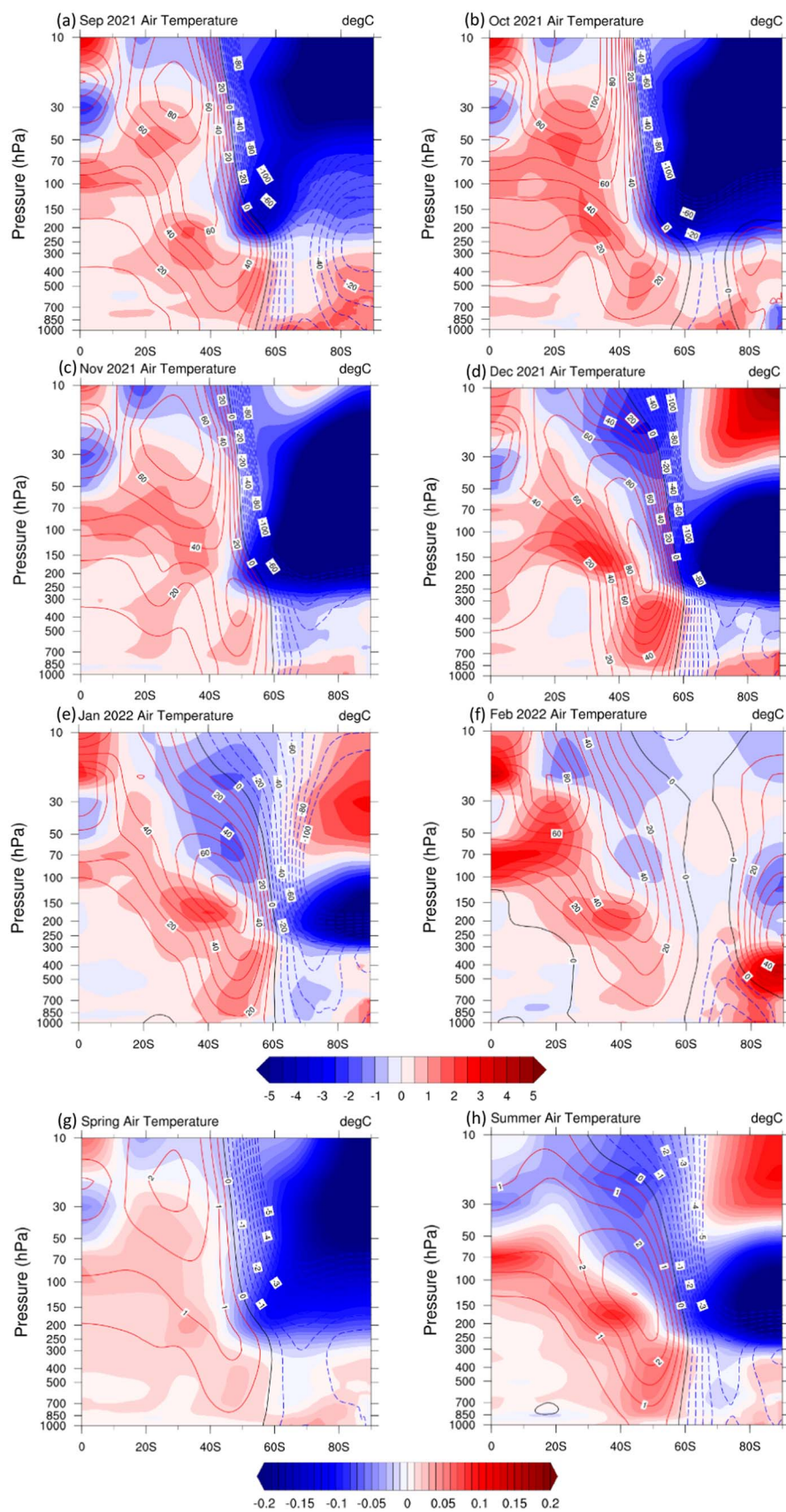
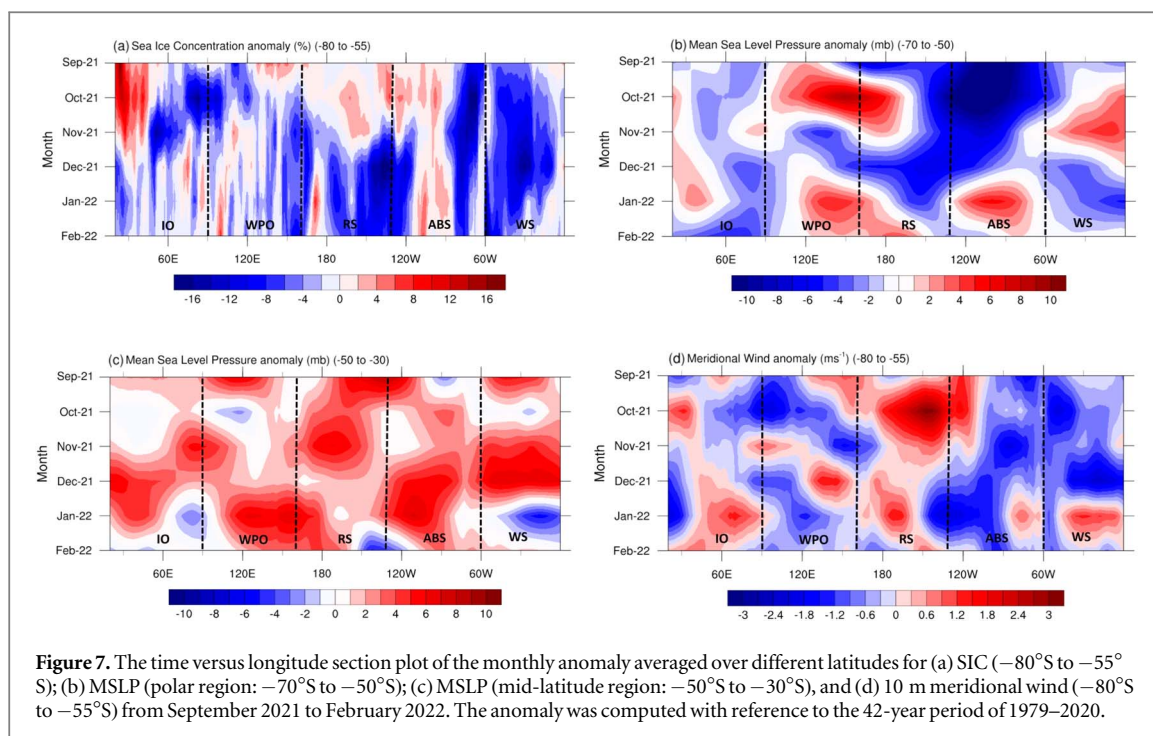


Figure 6. The zonal-mean monthly temperature ($^{\circ}\text{C}$) anomaly (shaded in colors) overlaid by the GPH anomaly (contour lines at 10 gpm interval) are shown in the vertical-latitude section from the equator to 90°S for (a) September 2021; (b) October 2021; (c) November 2021; (d) December 2021; (e) January 2022; (f) February 2022; (g) spring; and (h) summer. Anomalies were computed with reference to the 42-year period of 1979–2020.



surface and a negative anomaly above 850hPa over the Antarctic region (60°S – 90°S) in November. Therefore, it may be suggested that prolonged atmospheric warming on the surface beginning in September led to the maximum sea ice loss in November.

From December 2021 to February 2022, a negative SIC anomaly persisted across most Antarctic sectors (figures 3(d)–(f) and 7(a)). ASL set the lowest record (968 hPa) in December and the second-lowest record in February (figure 3(d)). Maximum growth and retreat of sea ice were observed in the Indian Ocean and Weddell Sea sectors, respectively. The intensification of westerlies drives cold surface waters off the Antarctic mainland and further sea ice advection northwards by Ekman transport (Hall and Visbeck 2002). This enhanced transport results in more northwards sea ice movement toward the northern Indian Ocean sector and the coastal Weddell Sea. Meanwhile, the increased poleward warmer wind flow regions corresponded to low sea ice, which was evident in the Ross Sea (figures 5(d), (e)). In January, the MSLP anomaly increased around the circumpolar trough from 60°S to 70°S , particularly in the western AP and ABS regions (figures 3(e) and 7(b)). This was reinforced by an increase in the magnitude of the zonal wave three (ZW3) pattern. It is an asymmetric pattern composed of three ridges close to 20°E , 90°E , and 150°W that affect climatic conditions and wind flow around the Antarctic coastal flank (Conolley 2002, Raphael 2004). The strong ZW3 pattern around Antarctica resembles a strong meridional flow with an alternate pattern of warm northerly, and cold southerly winds (Raphael 2007). Similarly, the earlier study found an association between the enhanced ZW3 states and the sea ice anomalies over the ABS sector (Irving and Simmonds 2015). The persistence of ZW3 contributes to sea ice retreat in the Ross Sea, western Weddell Sea, and the Indian Ocean, as well as sea ice advancement in the Bellingshausen Sea (figure 5(e)). The atmospheric temperature and GPH anomaly are also in agreement with the above findings (figures 6(d), (e)). In February, a positive temperature anomaly was observed extending from the surface to the upper atmosphere in the Antarctic region. Together, these mechanisms mentioned above may have set the ground for a new record of sea ice loss in February 2022. Unprecedented sea ice reductions are evident in figure 5(f), as there is little to no sea ice in most Antarctic regions. The positive SIC anomaly prevailed in the ABS sector in January, which decreased in the area once again, possibly due to the wind flow and warm air intrusion from the mid-latitudes in the previous month.

3.2.2. Seasonal variability

During spring 2021, a positive SIC anomaly persisted over the western ABS sector, Ross Sea, and the western Indian Ocean, while the rest of the sectors showed a negative SIC anomaly (figure 5(g)). The SIC anomaly pattern is consistent with the fifth-lowest Antarctic SIE in spring 2021 (figure 3(a)). The low sea ice in spring may be explained by a robust low-pressure center over the ABS sector and the deepening of the ASL (figure 5(g)). The anomalous westerlies towards the pole indicate a positive SAM, leading to SIC anomalies (Li *et al* 2018). In the Ross Sea and the western Indian Ocean, the prevailing wind flow pattern results in Ekman transport and hence the advection of sea ice northwards. However, a strong northerly wind results in sea ice retreat in the Weddell Sea. The temperature variation at different pressure levels in spring shows a weak positive anomaly in the higher

latitudes of the lower tropospheric region (figure 6(g)). In the Antarctic region, the GPH anomaly was negative from 300hPa to the upper stratosphere.

The second lowest Antarctic SIE was recorded in summer, close to the record low set in 2017 since satellite records began (figure 3(a)). The SIC anomaly is negative in the Ross Sea, western ABS, and the Weddell Sea. The equilibrium response of sea ice to climatic fluctuations in the previous season (month) is clear from the low summer sea ice record in summer (lowest in February) (figure 5). The positive SIC anomaly patch in the Indian Ocean, ABS sector, and the Weddell Sea was caused by the northwards advection of sea ice (figure 5(h)). In summer, a negative GPH anomaly center is observed in the Antarctic, which is bounded by the two positive temperature anomaly centers in the upper and lower atmosphere (figure 6(h)). At the same time, the positive surface temperature anomaly accelerates the sea ice loss towards higher latitudes.

4. Summary and conclusions

In this study, we analyzed monthly and seasonal SIE trends and the rate of change in sea ice across the entire Southern Ocean and its five sectors. These analyses were conducted across two distinct periods, 42-year (1979–2020) and 43/44 years (1979–2021/2022), to ascertain the influence of short-term monthly variability over longer periods. The Antarctic sea ice retreat from September 2021 was close to the minimum SIE records since 1979, with the lowest in February 2022. Seasonally, Antarctic SIE records reached the fifth lowest in spring 2021 and the second lowest during summer 2022. The anomalous sea ice retreat was in good agreement with the series of records observed for the climatic indices. The intensification of the low-pressure center in the Amundsen Sea and the positive SAM from September 2021 influence the wind patterns across the entire Southern Ocean. In addition, the PCH at 10 hPa and 50 hPa showed a strengthening of the stratospheric polar vortex with the lowest negative values. Thus, accelerating westerlies and inducing positive polarity of SAM. On the other hand, the ASL also deepens in association with the positive SAM index. The increased meridional flow of northerly winds contributed to the maximum spring sea ice retreat in the Bellingshausen Sea and Weddell Sea sectors. However, negative sea ice anomalies in the western Pacific Ocean are due to westerly flow. In October 2021, remarkable sea ice variation occurred in spring, possibly owing to the lowest ACP recorded since 1979. Positive sea ice anomalies towards the coastal area of the Antarctic mainland are related to northward sea ice advection due to Ekman transport. In December 2021, the fourth-highest positive SAM index and the lowest ACP resulted in an anomalous increase in westerlies across Antarctica and maximum negative sea ice anomalies. In contrast, a decrease in the MSLP anomaly around the circumpolar trough in January led to the ZW3 pattern. The existing pattern of MSLP anomalies contributed to the maximum sea ice recession in the Ross Sea, western Weddell Sea, and the Indian Ocean while advancing in the Bellingshausen Sea. Overall, the lowest Antarctic sea ice record in February 2022 resulted from the long months of sea ice retreat induced by the cumulative response of the positive SAM and the deepening of the ASL. Consistent with these observations, the atmospheric temperature and GPH anomaly also revealed evidence of warming at the surface, extending from the upper to the lower atmosphere and from the equator to the higher latitudes.

The findings of this study have implications for the future understanding of the role of atmospheric circulation and climate variability in driving specific short-term events of low Antarctic sea ice. The drivers of changes in the stratospheric polar vortex, SAM, ASL, wind, and pressure patterns over Antarctica are complex to understand. Due to the regional nature of Antarctic sea ice variability, small changes in atmospheric circulation in any sector may impact the SIE for the entire Southern Ocean. These findings indicate that ASL and SAM play a greater role in controlling sea ice variability in East Antarctica and the Weddell Sea during the ice retreat phase. The influence of the former on sea ice is determined by the amplitude of wind circulation and pressure patterns, as well as their direction and strength. This may provide insight into how Antarctic sea ice evolved before the satellite era and how it may vary in the future.

Acknowledgments

We gratefully acknowledge the Director, National Centre for Polar and Ocean Research (NCPOR) and Ministry of Earth Sciences (MoES), New Delhi, for continuous support. Juhi Yadav thanks the University Grants Commission (UGC), New Delhi, India, for the Senior Research Fellowship Award. The authors sincerely acknowledge various organizations, such as the National Snow and Ice Data Center (NSIDC), National Oceanic and Atmospheric Administration (NOAA), Copernicus Marine Environment Monitoring Service, National Centre for Atmospheric Research (NCAR), Technische Universität Dresden, and the Polar Science Center, Applied Physics Laboratory, for providing various datasets available in their portals. We thank the editor and anonymous reviewers for their thorough review and constructive comments. This is NCPOR contribution no J- 48/2022–23.

Data availability statement

Daily and seasonal sea ice extent data for the total Antarctic and its five sectors are obtained from U.S. National Snow and Ice Data Center based on Bootstrap and NASA algorithm (available at https://daacdata.apps.nsidc.org/pub/DATASETS/nsidc0192_seaice_trends_climo_v3/total-ice-area-extent/). We acknowledge the European Centre for Medium-range Weather Forecasts for providing the higher spatiotemporal resolution fifth-generation reanalysis monthly data at single and pressure levels for sea ice concentration, mean sea level pressure, 10 m zonal and meridional wind components, geopotential height, and temperature (available at <https://cds.climate.copernicus.eu/cdsapp#!/dataset/reanalysis-era5-single-levels-monthly-means?tab=overview> and <https://cds.climate.copernicus.eu/cdsapp#!/dataset/reanalysis-era5-pressure-levels-monthly-means?tab=overview>). The monthly data of the Amundsen Sea Low Actual Central Pressure index (https://scotthosking.com/asl_index) and Southern Annular Mode index (<https://legacy.bas.ac.uk/met/gjma/sam.html>) were obtained from National Center for Atmospheric Research.

ORCID iDs

Juhi Yadav  <https://orcid.org/0000-0002-4575-7942>

Avinash Kumar  <https://orcid.org/0000-0002-6511-8435>

Rahul Mohan  <https://orcid.org/0000-0001-8758-2215>

References

- Abram N J, Mulvaney R, Vimeux F, Phipps S J, Turner J and England M H 2014 Evolution of the Southern Annular Mode during the past millennium *Nat. Clim. Chang.* **4** 564–9
- Arblaster J M and Meehl G A 2006 Contributions of External Forcings to Southern Annular Mode Trends **19** 2896–2905
- Armour K C, Marshall J, Scott J R, Donohoe A and Newsom E R 2016 Southern Ocean warming delayed by circumpolar upwelling and equatorward transport *Nat. Geosci.* **9** 549–54
- Bintanja R, Van Oldenborgh G J, Drijfhout S S, Wouters B and Katsman C A 2013 Important role for ocean warming and increased ice-shelf melt in Antarctic sea-ice expansion *Nat. Geosci.* **6** 376–9
- Bromwich D H, Nicolas J P, Monaghan A J, Lazzara M A, Keller L M, Weidner G A and Wilson A B 2012 Central West Antarctica among the most rapidly warming regions on Earth *Nat. Geosci.* **6** 139–45
- Cavalieri D J and Parkinson C L 2012 Arctic sea ice variability and trends, 1979–2010 *Cryosphere* **6** 881–9
- Cavalieri D J, Parkinson C L, Gloersen P and Zwally H J 1996 Sea Ice concentrations from Nimbus-7 SMMR and DMSP SSM/I-SSMIS passive microwave data, version 1. [NSIDC-0051] Natl. Snow Ice Data Center. Boulder, Color. USA 0-29
- Cavalieri D J, Parkinson C L and Vinnikov K Y 2003 30-year satellite record reveals contrasting Arctic and Antarctic decadal sea ice variability *Geophys. Res. Lett.* **30**
- Cerrone D, Fusco G, Simmonds I, Aulicino G and Budillon G 2017 Dominant covarying climate signals in the southern ocean and antarctic sea ice influence during the last three decades *J. Clim.* **30** 3055–72
- Comiso J C, Gersten R A, Stock L V, Turner J, Perez G J and Cho K 2017 Positive trend in the Antarctic sea ice cover and associated changes in surface temperature *J. Clim.* **30** 2251–67
- Connolley W M 2002 Long-term variation of the Antarctic Circumpolar Wave *J. Geophys. Res. Ocean.* **107** SOV 3–1
- Djoumna G and Holland D M 2021 Atmospheric rivers, warm air intrusions, and surface radiation balance in the amundsen sea embayment *J. Geophys. Res. Atmos.* **126** e2020JD034119
- Doddridge E W and Marshall J 2017 Modulation of the seasonal cycle of antarctic sea ice extent related to the Southern Annular Mode *Geophys. Res. Lett.* **44** 9761–8
- Donat-Magnin M, Jourdain N C, Gallée H, Amory C, Kittel C, Fettweis X, Wille J D, Favier V, Drira A and Agosta C 2020 Interannual variability of summer surface mass balance and surface melting in the Amundsen sector, West Antarctica *Cryosphere* **14** 229–49
- Eayrs C, Holland D, Francis D, Wagner T, Kumar R and Li X 2019 Understanding the seasonal cycle of antarctic sea ice extent in the context of longer-term variability *Rev. Geophys.* **57** 1037–64
- Eayrs C, Li X, Raphael M N and Holland D M 2021 Rapid decline in Antarctic sea ice in recent years hints at future change *Nat. Geosci.* **14** 460–4
- England M R, Shaw T A and Polvani L M 2016 Troposphere-stratosphere dynamical coupling in the southern high latitudes and its linkage to the Amundsen Sea *J. Geophys. Res. Atmos.* **121** 3776–89
- Fogt R L, Sleinkofer A M, Raphael M N and Handcock M S 2022 A regime shift in seasonal total Antarctic sea ice extent in the twentieth century *Nat. Clim. Chang.* **12** 54–62
- Fogt R L, Wovrosh A J, Langen R A and Simmonds I 2012 The characteristic variability and connection to the underlying synoptic activity of the Amundsen-Bellingshausen Seas Low *J. Geophys. Res. Atmos.* **117**
- Hall A and Visbeck M 2002 Synchronous variability in the Southern Hemisphere atmosphere, sea ice, and ocean resulting from the annular mode *J. Clim.* **15** 3043–57
- Hersbach H *et al* 2020 The ERA5 global reanalysis *Q. J. R. Meteorol. Soc.* **146** 1999–2049
- Holland M M, Landrum L, Kostov Y and Marshall J 2017 Sensitivity of Antarctic sea ice to the Southern Annular Mode in coupled climate models *Clim. Dyn.* **49** 1813–31
- Holland M M, Landrum L, Raphael M N and Kwok R 2018 The regional, seasonal, and lagged influence of the Amundsen Sea Low on Antarctic Sea Ice *Geophys. Res. Lett.* **45** 227–11
- Hosking J S, Orr A, Marshall G J, Turner J and Phillips T 2013 The influence of the Amundsen–Bellingshausen seas low on the climate of West Antarctica and its representation in coupled climate model simulations *J. Clim.* **26** 6633–48
- Irving D and Simmonds I 2015 A novel approach to diagnosing Southern hemisphere planetary wave activity and its influence on regional climate variability *J. Clim.* **28** 9041–57

- Kumar A, Yadav J and Mohan R 2021 Seasonal sea-ice variability and its trend in the Weddell Sea sector of West Antarctica *Environ. Res. Lett.* **16** 24046
- Kusahara K, Reid P, Williams G D, Massom R and Hasumi H 2018 An ocean-sea ice model study of the unprecedented Antarctic sea ice minimum in 2016 *Environ. Res. Lett.* **13** 084020
- Lee S, Gong T, Feldstein S B, Screen J A and Simmonds I 2017 Revisiting the Cause of the 1989–2009 arctic surface warming using the surface energy budget: downward infrared radiation dominates the surface fluxes *Geophys. Res. Lett.* **44** 654–10
- Li F, Orsolini Y J, Wang H, Gao Y and He S 2018 Atlantic multidecadal oscillation modulates the impacts of Arctic sea ice decline *Geophys. Res. Lett.* **45** 2497–506
- Lim E-P and Simmonds I 2002 Explosive cyclone development in the Southern Hemisphere and a comparison with Northern Hemisphere events *Mon. Weather Rev.* **130** 2188–209
- Marshall G J 2003 Trends in the Southern annular mode from observations and reanalyses *J. Clim.* **16** 4134–43
- Meehl G A, Arblaster J M, Chung C T Y, Holland M M, DuVivier A, Thompson L A, Yang D and Bitz C M 2019 Sustained ocean changes contributed to sudden Antarctic sea ice retreat in late 2016 *Nat. Commun.* **10**
- NSIDC 2004 DMSP SSM/I-SSMIS Daily Polar Gridded Brightness Temperatures, Version 4 How to Cite These Data 0–26
- Parkinson C L 2019 A 40-y record reveals gradual Antarctic sea ice increases followed by decreases at rates far exceeding the rates seen in the Arctic *Proc. Natl. Acad. Sci. U. S. A.* **116** 14414–23
- Parkinson C L and Cavalieri D J 2012 Antarctic sea ice variability and trends, 1979–2010 *Cryosphere* **6** 871–80
- Parkinson C L, Cavalieri D J, Gloersen P, Zwally H J and Comiso J C 1999 Arctic sea ice extents, areas, and trends, 1978–1996 *J. Geophys. Res. Ocean.* **104** 20837–56
- Pezza A B, Rashid H A and Simmonds I 2012 Climate links and recent extremes in antarctic sea ice, high-latitude cyclones, Southern Annular Mode and ENSO *Clim. Dyn.* **38** 57–73
- Purich A, England M H, Cai W, Sullivan A and Durack P J 2018 Impacts of broad-scale surface freshening of the Southern Ocean in a coupled climate model *J. Clim.* **31** 2613–32
- Raphael M N 2004 A zonal wave 3 index for the Southern Hemisphere *Geophys. Res. Lett.* **31** 1–4
- Raphael M N 2007 The influence of atmospheric zonal wave three on Antarctic sea ice variability *J. Geophys. Res. Atmos.* **112**
- Raphael M N and Hancock M S 2022 A new record minimum for Antarctic sea ice *Nat. Rev. Earth Environ.* **3** 215–6
- Raphael M N, Holland M M, Landrum L and Hobbs W R 2019 Links between the Amundsen Sea Low and sea ice in the Ross Sea: seasonal and interannual relationships *Clim. Dyn.* **52** 2333–49
- Sato K and Simmonds I 2021 Antarctic skin temperature warming related to enhanced downward longwave radiation associated with increased atmospheric advection of moisture and temperature *Environ. Res. Lett.* **16** 064059
- Screen J A, Bracegirdle T J and Simmonds I 2018 Polar climate change as manifest in atmospheric circulation *Curr. Clim. Chang. Reports* **4** 383–95
- Serreze M C, Maslanik J A, Scambos T A, Fetterer F, Stroeve J, Knowles K, Fowler C, Drobot S, Barry R G and Haran T M 2003 A record minimum arctic sea ice extent and area in 2002 *Geophys. Res. Lett.* **30** 1110
- Siegmund P 2005 Stratospheric polar cap mean height and temperature as extended-range weather predictors *Mon. Weather Rev.* **133** 2436–48
- Simmonds I 2015 Comparing and contrasting the behaviour of Arctic and Antarctic sea ice over the 35 year period 1979–2013 *Ann. Glaciol.* **56** 18–28
- Simmonds I and Li M 2021 Trends and variability in polar sea ice, global atmospheric circulations, and baroclinicity *Ann. N. Y. Acad. Sci.* **1504** 167–86
- Simmonds I and Wu X 1993 Cyclone behaviour response to changes in winter southern hemisphere sea-ice concentration *Q. J. R. Meteorol. Soc.* **119** 1121–48
- Stuecker M F, Bitz C M and Armour K C 2017 Conditions leading to the unprecedented low Antarctic sea ice extent during the 2016 austral spring season *Geophys. Res. Lett.* **44** 9008–19
- Tetzner D, Thomas E and Allen C 2019 A validation of ERA5 reanalysis data in the southern antarctic peninsula—Ellsworth land region, and its implications for ice core studies *Geosci.* **9** 289
- Thompson D W J and Wallace J M 2000 Annular modes in the extratropical circulation. Part I : month-to-month variability *J. Clim.* **13** 1000–16
- Turner J, Holmes C, Harrison T C, Phillips T, Jena B, Reeves-Francois T, Fogt R, Thomas E R and Bajish C C 2022 Record low antarctic sea ice cover in february 2022 *Geophys. Res. Lett.* **49** e2022GL098904
- Turner J, Hosking J S, Bracegirdle T J, Marshall G J and Phillips T 2015 Recent changes in Antarctic Sea Ice *Philos. Trans. R. Soc. A Math. Phys. Eng. Sci.* **373**
- Turner J and Overland J 2009 Contrasting climate change in the two polar regions *Polar Res.* **28** 146–64
- Turner J, Phillips T, Hosking J S, Marshall G J and Orr A 2013 The Amundsen Sea low *Int. J. Climatol.* **33** 1818–29
- Turner J, Phillips T, Marshall G J, Hosking J S, Pope J O, Bracegirdle T J and Deb P 2017 Unprecedented springtime retreat of Antarctic sea ice in 2016 *Geophys. Res. Lett.* **44** 6868–75
- Wang G, Hendon H H, Arblaster J M, Lim E P, Abhik S and van Renshu P 2019 Compounding tropical and stratospheric forcing of the record low Antarctic sea-ice in 2016 *Nat. Commun.* **10** 1–9
- Wang S, Liu J, Cheng X, Kerzenmacher T, Hu Y, Hui F and Braesicke P 2021 How do weakening of the stratospheric polar vortex in the Southern Hemisphere affect regional antarctic sea ice extent? *Geophys. Res. Lett.* **48**
- Yeung Y, Yiu S and Maycock A C 2019 On the Seasonality of the El Niño teleconnection to the Amundsen sea region *J. Clim.* **32** 4829–45
- Zhang L, Gan B, Li X, Wang H, Wang C Y, Cai W and Wu L 2021 Remote influence of the midlatitude South Atlantic variability in spring on Antarctic summer sea ice *Geophys. Res. Lett.* **48** 2020GL090810
- Zwally H J, Comiso J C, Parkinson C L, Cavalieri D J and Gloersen P 2002 Variability of Antarctic sea ice 1979–1998 *J. Geophys. Res. Ocean.* **107** 9–1